Published Online First on October 20, 2009 as 10.1158/0008-5472.CAN-09-1067

# Deletion of PTEN Promotes Tumorigenic Signaling, Resistance to Anoikis, and Altered Response to Chemotherapeutic Agents in Human Mammary Epithelial Cells

**Michele I. Vitolo,[1] Michele B. Weiss,[1,2] Marta Szmacinski,[3] Khola Tahir,[1,4] Todd Waldman,[6] Ben Ho Park,[5] Stuart S. Martin,[1] David J. Weber,[1,3] and Kurtis E. Bachman[1,3]**

[1]University of Maryland Greenebaum Cancer Center; [2]University of Maryland Graduate Program in Molecular Medicine; Departments of [3]Biochemistry and Molecular Biology and [4]Radiation Oncology, University of Maryland School of Medicine; [5]The Sidney Kimmel Comprehensive Cancer Center at Johns Hopkins, Department of Oncology, The Johns Hopkins University School of Medicine, Baltimore, Maryland; and [6]Lombardi Comprehensive Cancer Center, Georgetown University School of Medicine, Washington, District of Columbia

## Abstract

**Many cancers, including breast cancer, harbor loss-of-function mutations in the catalytic domain of phosphatase and tensin homologue deleted on chromosome 10 (PTEN) or have reduced PTEN expression through loss of heterozygosity and/or epigenetic silencing mechanisms. However, specific phenotypic effects of PTEN inactivation in human cancer cells remain poorly defined without a direct causal connection between the loss of PTEN function and the development or progression of cancer. To evaluate the biological and clinical relevance of reduced or deleted PTEN expression, a novel *in vitro* model system was generated using human somatic cell knockout technologies. Targeted homologous recombination allowed for a single and double allelic deletion, which resulted in reduced and deleted PTEN expression, respectively. We determined that heterozygous loss of PTEN in the nontumorigenic human mammary epithelial cell line MCF-10A was sufficient for activation of the phosphoinositide 3-kinase/AKT and mitogen-activated protein kinase pathways, whereas the homozygous absence of PTEN expression led to a further increased activation of both pathways. The deletion of PTEN was able to confer growth factor–independent proliferation, which was confirmed by the resistance of the *PTEN*$^{-/-}$ MCF-10A cells to small-molecule inhibitors of the epidermal growth factor receptor. However, neither heterozygous nor homozygous loss of PTEN expression was sufficient to promote anchorage-independent growth, but the loss of PTEN did confer apoptotic resistance to cell rounding and matrix detachment. Finally, MCF-10A cells with the reduction or loss of PTEN showed increased susceptibility to the chemotherapeutic drug doxorubicin but not paclitaxel.** [Cancer Res 2009;69(21):8275–83]

## Introduction

Phosphatase and tensin homologue deleted on chromosome 10 (*PTEN*) is a tumor suppressor gene that dephosphorylates phosphatidylinositol 3,4,5-trisphosphate, the product of the lipid kinase phosphoinositide 3-kinase (PI3K). PTEN antagonizes activated PI3K to maintain normal cell growth or arrest, survival, or apoptosis. PTEN and PI3K exist in a tight regulatory loop, and a reduction or deletion of PTEN or the acquisition of an activating mutation in PI3K leads to abnormal activation of the PI3K pathway.

*PTEN* is the second most frequently mutated gene in human cancers following *TP53*. Immunohistochemistry studies of tumors from breast, pancreatic, and ovarian cancers have shown a loss of PTEN protein in 30% to 50% of samples (1–5). In breast cancer, this loss correlates highly with lymph node metastasis (5). Additionally, germ-line mutations in the *PTEN* gene are associated with multineoplastic, autosomally dominant human syndromes such as Cowden's disease and Bannayan-Zonana syndrome. Each syndrome features a predisposition to the formation of different malignancies, including breast cancer in 20% to 50% of the affected females (6, 7). The high frequency of reduction or loss of PTEN in breast cancer suggests its potential role in initiation and/or progression of human breast cancer.

Previously, the effects of PTEN loss have primarily been measured in tumor cell lines, which harbor numerous other transforming and oncogenic mutations. This has made it difficult to determine which phenotypes are directly conferred by the loss of PTEN and to define the stages of tumorigenesis that are specifically altered in cells with PTEN loss. To elucidate the connection between PTEN loss and the initiation and/or progression of human breast carcinomas, somatic cell gene targeting technology was used to more closely mimic the physiologic reduction or loss of PTEN in epithelial cells. This *in vitro* model system involved targeted homologous recombination to disrupt each allele of *PTEN* in the nontumorigenic mammary epithelial cell (MEC) line, MCF-10A. Using these isogenic somatic cell *PTEN* knockout lines, we determined that PTEN loss induces not only the activation of the PI3K pathway but also the mitogen-activated protein kinase (MAPK) pathway. This increase in pathway activation led to growth factor–independent proliferation that was suppressed with either PI3K or MAPK inhibitors. PTEN loss in MCF-10A cells also increased anchorage-independent survival but was insufficient to confer anchorage-independent growth. Also, of potential clinical importance, PTEN loss confers susceptibility to the chemotherapeutic drug, doxorubicin, but not paclitaxel, two agents commonly used for breast cancer therapy.

## Materials and Methods

**Cell lines and cell culture.** MCF-10A cells were purchased from the American Type Culture Collection and maintained as described previously

---

**Note:** Supplementary data for this article are available at Cancer Research Online (http://cancerres.aacrjournals.org/).

**Requests for reprints:** Kurtis E. Bachman, GlaxoSmithKline, 709 Swedeland Road, UW2109, King of Prussia, PA 19406. Phone: 610-270-6045; Fax: 610-270-5598; E-mail: kurtis.e.bachman@gsk.com; Michele I. Vitolo, University of Maryland Greenebaum Cancer Center, 655 West Baltimore Street, Baltimore, MD 21201. Phone: 410-706-4142; Fax: 410-706-7619; E-mail: mvitolo@umaryland.edu; and David J. Weber, University of Maryland School of Medicine, 108 North Greene Street, Baltimore, MD 21201. Phone: 410-706-4354; Fax: 410-706-0458; E-mail: dweber@umaryland.edu.

©2009 American Association for Cancer Research.

doi:10.1158/0008-5472.CAN-09-1067

(8) supplemented with 0.1 μg/mL cholera toxin. Minimal assay medium was composed of DMEM/F-12 without phenol red, 1% charcoal stripped dextran–treated fetal bovine serum (Hyclone), and 100 units/mL penicillin-streptomycin without exogenous growth factors. MCF-10A.Bcl2 cells were created by stable transfection with the pBP/Bcl2 expression vector (9) and maintained in MCF-10A growth medium supplemented with 2.5 μg/mL puromycin. Cells were maintained in a 37°C incubator with 5% $CO_2$.

***PTEN*$^{+/-}$ and *PTEN*$^{-/-}$ cell line generation.** Heterozygote clones were created as described previously (10). A second construct was generated to delete exon 2 of *PTEN* on the second allele. Briefly, sequences with exact homology to intronic regions flanking exon 2 were cloned into the pAAV-MCS (Stratagene) via the pSept vector (11, 12). The adeno-associated virus was generated using the AAV Helper-free system from Stratagene following the manufacturer's instructions. Individual G418-resistant clones were tested via PCR for the presence of a homozygote *PTEN* knockout. Positive clones were treated with a Cre recombinase virus to excise the *IRES-neo*$^R$ gene. Cells were maintained in MCF-10A growth medium as described above.

**Proliferation assays.** Cell were seeded in quadruplicate at $2.0 \times 10^3$ per well in 96-well plates in minimal assay medium. The next day, the appropriate medium with or without drug was added. Cell viability was quantified using MTT (Sigma). After MTT treatment, the medium was removed, the converted dye was solubilized in 0.01 mol/L glycine in DMSO, and the absorbance (450 nm) was measured. For growth in the absence of drugs, a set of cells were exposed to MTT on day 0 to accurately assess starting cell number. Growth was calculated as a percent above cell number on day 0. For the erlotinib and gefitinib (LC Laboratories) studies, untreated wells of each cell line were used as the control of calculation percent viability.

**Western blot analysis.** Cell lysates were prepared in radioimmunoprecipitation assay lysis buffer [0.5 mol/L Tris-HCl (pH 7.4), 1.5 mol/L NaCl, 2.5% deoxycholic acid, 10% NP-40, 10 mmol/L EDTA] supplemented with protease inhibitor cocktail EDTA-free (Roche) and phosphatase inhibitor cocktail II (Calbiochem). Western blotting was done using NuPage gels (Invitrogen). Primary antibodies for PTEN, pAKT (S473), AKT, phosphorylated extracellular signal-regulated kinase 1/2 (pERK1/2), ERK1/2, and poly(ADP-ribose) polymerase (PARP; Cell Signaling) and glyceraldehyde-3-phosphate dehydrogenase (Abcam) were used at the manufacturers' recommended dilutions.

**Flow cytometry.** For sub-$G_1$ analysis, cells were ethanol-fixed and treated with RNase A (1 mg/mL) and propidium iodide (20 μg/mL). Cells were analyzed by a Becton Dickinson LSR-II at the Flow Cytometry Core Laboratory, CVD Immunology Group at the University of Maryland.

**Survival assays.** Cell were seeded in quadruplicate at $1.5 \times 10^4$ per well in 96-well plates in minimal assay medium. The next day, the appropriate concentrations of doxorubicin (Calbiochem) or paclitaxel (Invitrogen) were added to the cells. On day 5, cell viability was quantified using MTT. Untreated wells of each cell line were used as the control of calculation percent viability.

## Results

***PTEN* heterozygous and homozygous loss promotes activation of both PI3K and MAPK pathways in MECs.** Reduction of PTEN expression or complete loss is observed in ~40% of human breast cancers (2, 5, 13). To determine the oncogenic phenotype of reduced or absent *PTEN* expression in human breast epithelial cells, we generated isogenic human MECs using MCF-10A cells. MCF-10A breast epithelial cells were chosen for targeted *PTEN* knockout because these cells are human, mostly diploid, nontumorigenic cell line and karyotype analysis of late-passage cells show genetic stability (data not shown). The use of nontumorigenic cell lines allows us to assess any oncogenic effects directly resulting from loss of *PTEN*. Several independently derived heterozygous knockout clones (*PTEN*$^{+/-}$) were identified containing one active *PTEN* allele. Subsequent targeting of the second allele was accomplished to yield homozygous *PTEN* (*PTEN*$^{-/-}$) knockout clones.

Somatic cell gene knockout was accomplished via homologous recombination between the genomic locus and the targeting vector to delete exon II of *PTEN* and replace it with a promoterless, *IRES-neo*$^R$ gene flanked by *LoxP* sites (Fig. 1*A*). For each round of targeting, positive clones were verified by PCR. Subsequent removal of the *IRES-neo*$^R$ cassette was accomplished by treatment with Cre recombinase. At least three single, independent isogenic *PTEN*$^{+/-}$ and *PTEN*$^{-/-}$ clones from separate infections were isolated and used to account for any clonal variations.

MCF-10A *PTEN*$^{+/-}$ clones showed a decrease in PTEN levels (Fig. 1*B, lanes 2-4*) and *PTEN*$^{-/-}$ clones completely lacked PTEN expression (Fig. 1*B, lanes 5-7*). The absence of PTEN mRNA in *PTEN*$^{-/-}$ clones was verified by real-time PCR (data not shown). All *PTEN*$^{-/-}$ clones maintained increased pAKT levels over their *PTEN*$^{+/-}$ and parental counterparts. Interestingly, activated ERK (pERK1/2) levels were also increased in *PTEN*$^{-/-}$ clones over the MCF-10A parental cells. Although *PTEN*$^{+/-}$ clones showed an increase in activated ERK levels from the parental cells, the increase was less dramatic or consistent among *PTEN*$^{+/-}$ clones (Fig. 1*B*). However, in conjunction with an increase in pERK1/2 in *PTEN*$^{-/-}$ clones, decreased total ERK levels were consistently observed.

**PTEN loss confers growth factor–independent proliferation.** To determine whether the activation of the PI3K and MAPK pathways altered proliferation rates, MCF-10A, *PTEN*$^{+/-}$, and *PTEN*$^{-/-}$ clones were analyzed over a period of 9 days. Interestingly, at early passage, *PTEN*$^{+/-}$ and *PTEN*$^{-/-}$ clones with reduced or deleted PTEN grew significantly slower than parental MCF-10A cells (Fig. 2*A*; $P < 0.05$), whereas, at later passage, MCF-10A cells maintain a similar growth rate to that of their earlier-passage counterparts; the proliferation rates of *PTEN*$^{+/-}$ and *PTEN*$^{-/-}$ clones increase over time (Fig. 2*A*). The parental MCF-10A, *PTEN*$^{+/-}$, and *PTEN*$^{-/-}$ clones do not undergo any significant cell death over the first 7 days due to the absence of a sub-$G_1$ population (Supplementary Fig. S1). However, once the cells achieve contact inhibition by day 7, all cells begin to die as shown by a drop in viability and the presence of a sub-$G_1$ peak. The increase proliferation rate is likely due to a variety of mechanisms downstream of AKT activation, such as increased cyclin D1 expression, inhibition of forkhead transcription factors, or reduction of $p27^{Kip1}$, all of which positively regulate $G_1$-S cell cycle progression (reviewed in ref. 14).

A well-known characteristic of MCF-10A MECs is their epidermal growth factor (EGF) requirement for cellular proliferation. Growth factor–independent proliferation is a common hallmark in cancer cells containing oncogenic phenotypes and aberrantly activated signaling (15). Because *PTEN*$^{+/-}$ and *PTEN*$^{-/-}$ clones have an increase in activated PI3K and MAPK pathways, we examined whether the increased activation of these pathways was sufficient to confer EGF-independent growth by treating the cells with increasing concentrations of the clinically administered EGF receptor small-molecule inhibitors gefitinib and erlotinib (Fig. 2*B*). Compared with the parental and *PTEN*$^{+/-}$ clones, *PTEN*$^{-/-}$ clones were significantly more resistant to growth inhibition via the EGF receptor inhibitors, indicating a decreased requirement of EGF for proliferation. To confirm this observation, MCF-10A cells and *PTEN*$^{+/-}$ and *PTEN*$^{-/-}$ clones were maintained in minimal assay medium devoid of exogenous growth factors for 9 days. As observed previously using compounds to disrupt EGF signaling, MCF-10A cells and *PTEN*$^{+/-}$ clones showed reduced growth (Fig. 2*C*). However, *PTEN*$^{-/-}$ cells survived and continued to slowly proliferate although considerably slower than in medium supplemented with EGF. At later passage, *PTEN*$^{-/-}$ cell proliferation in the absence of mitogens became more robust (Supplementary Fig. S2).

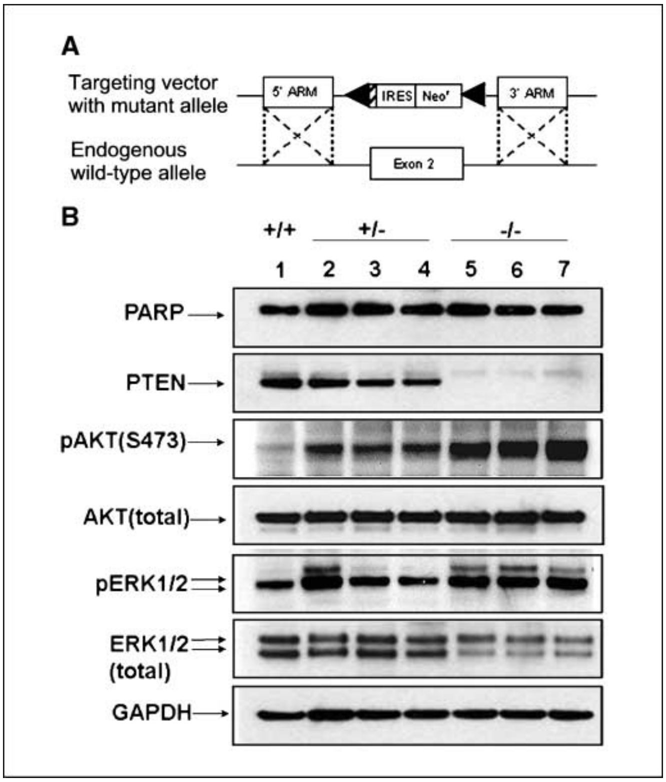

**Figure 1.** Single and biallelic deletion of the *PTEN* gene. *A,* to remove each copy of *PTEN*, our targeting construct contained a neomycin resistance cassette flanked by LoxP sites and homologous sequences to the intronic regions 5′ and 3′ of exon 2. *B,* MCF-10A cells (*lane 1*) and *PTEN*$^{+/-}$ (*lanes 2-4*) and *PTEN*$^{-/-}$ (*lanes 5-7*) clones were harvested at subconfluence during exponential growth. PTEN expression is reduced in *PTEN*$^{+/-}$ clones and absent in *PTEN*$^{-/-}$ clones. With a reduction and deletion of PTEN, activated AKT (pAKT) is increased (*top bands*), whereas total AKT levels remain equivalent. Activated ERK (pERK1/2) levels are also increased in the clones. Glyceraldehyde-3-phosphate dehydrogenase (*GAPDH*) was used as a loading control.

Immunoblots confirmed the increased activity of each pathway in the presence and absence of mitogens (Fig. 2*D*). After 24 h in growth medium, the levels of pAKT are highest in *PTEN*$^{-/-}$ clones and slightly more elevated in *PTEN*$^{+/-}$ clones compared with the MCF-10A parental cells. Assessment of the same set of cells grown in medium without mitogens showed reduced levels of pAKT. Although there is a minimal level of detectable pAKT in the parental and *PTEN*$^{+/-}$ clones, *PTEN*$^{-/-}$ clones continue to maintain elevated pAKT levels at 24, 48, and 72 h.

pERK levels were also slightly elevated in all *PTEN*$^{+/-}$ and *PTEN*$^{-/-}$ clones compared with the MCF-10A parental cells when grown in normal culture medium (Fig. 2*D*). The levels of activated ERK were similar between *PTEN*$^{+/-}$ and *PTEN*$^{-/-}$ clones. This result differed from the earlier immunoblot results (Fig. 1*B*) likely due to different harvest times after replating. Cells in Fig. 1*B* were harvested during exponential growth 3 days after replating, whereas cells in Fig. 2*D* were harvested only 24 h after replating when they are not yet in exponential growth. However, after 3 days in medium devoid of growth factors, *PTEN*$^{+/-}$ cells have increased pERK levels over the MCF-10A parental cells, and *PTEN*$^{-/-}$ cells have pERK levels higher than *PTEN*$^{+/-}$ clones, similar to the pattern of ERK phosphorylation seen after 3 days in culture medium (Fig. 1*B*). This pattern of increasing levels of activated ERK, from MCF-10A parental cells to their *PTEN*$^{-/-}$ isogenic counterparts, indicates that, even under growth factor–reduced conditions, loss of PTEN allows for activation of the ERK signaling pathway.

To determine if the improved cell growth in *PTEN*$^{-/-}$ cells resulted from differences in cell cycling or reduced apoptosis, we performed flow cytometry measurements of DNA content throughout the growth in minimal medium (Fig. 3). These results showed that both MCF-10A and *PTEN*$^{+/-}$ cells undergo apoptotic DNA cleavage beginning on day 3 that increases to 87% and 81%, respectively, by day 9, whereas *PTEN*$^{-/-}$ cells show no signs of apoptosis. The increased viability of *PTEN*$^{-/-}$ cells is primarily from resistance to apoptosis rather than a difference in cell cycling. The elevation of apoptosis in MCF-10A and *PTEN*$^{+/-}$ cells during exposure to minimal medium is clearly sufficient to offset any cell growth and keep the cell population from increasing.

**Growth factor–independent proliferation due to PTEN loss can be inhibited by pharmacologic blockade of PI3K and MAPK pathways.** To confirm the requirement of active PI3K and MAPK pathways for continued cell proliferation in the absence of growth factors, *PTEN*$^{-/-}$ cells were treated with inhibitors of each pathway and growth factor–independent proliferation was assessed. Only *PTEN*$^{-/-}$ cells were used in this experiment because the parental and heterozygote clones do not grow under these conditions (Fig. 2*C*). Increasing concentrations of the PI3K inhibitor, LY294002, in minimal assay medium was added to the cells, and after 5 days, a dose-dependent inhibition of growth was observed. The addition of 10 μmol/L LY294002 led to nearly complete inhibition of proliferation of all *PTEN*$^{-/-}$ clones (Fig. 4*A*). Similarly, *PTEN*$^{-/-}$ clones were grown in the presence of the MEK1/2 inhibitor, U0126 (Fig. 4*B*). There was also a dose-dependent growth inhibition of *PTEN*$^{-/-}$ cells following exposure to the MEK inhibitor. In the presence of 1 μmol/L U0126, growth factor–independent proliferation was inhibited by >50% and almost completely inhibited with 2.5 μmol/L U0126.

To verify inhibition of the PI3K and MAPK pathways by LY294002 and U0126, respectively, immunoblots were done. In the absence of the PI3K or MEK1/2 inhibitors, *PTEN*$^{-/-}$ clones displayed high levels of pAKT and pERK (Fig. 4*A*). After LY294002 treatment, all *PTEN*$^{-/-}$ clones showed a significant drop in pAKT levels. Following U0126 treatment, the levels of pERK dropped to almost undetectable levels.

**Anchorage-independent survival and growth.** Because PTEN loss highly correlates with increased breast cancer lymph node metastasis (16–18), it was next determined if PTEN loss alone would lead to the transformation of nontumorigenic breast epithelial cells. Anchorage-independent growth in soft agar is a property of transformed cells that best correlates with *in vivo* tumorigenicity (19). MCF-10A nontumorigenic parental cells and *PTEN*$^{-/-}$ clones were plated in soft agar and incubated for 21 days. MCF-7 breast cancer line was used as a positive control for colony growth and only incubated for 14 days due to the formation of multiple, large colonies. As expected, MCF-10A cells did not form colonies. Likewise, *PTEN*$^{-/-}$ cells were unable to form colonies in soft agar and unable to form tumors in severe combined immunodeficient mice ($n = 5$) after 24 weeks (data not shown). However, colony formation in soft agar and *in vivo* tumor growth rely on anchorage-independent proliferation but are not a sufficient test for increased resistance to anoikis or apoptosis after matrix detachment. Because previous data have shown that activation of the PI3K pathway contributes to cell survival after detachment (20), MCF-10A, *PTEN*$^{+/-}$, and *PTEN*$^{-/-}$ cells were next tested for apoptotic resistance during cell rounding and detachment. Included in these

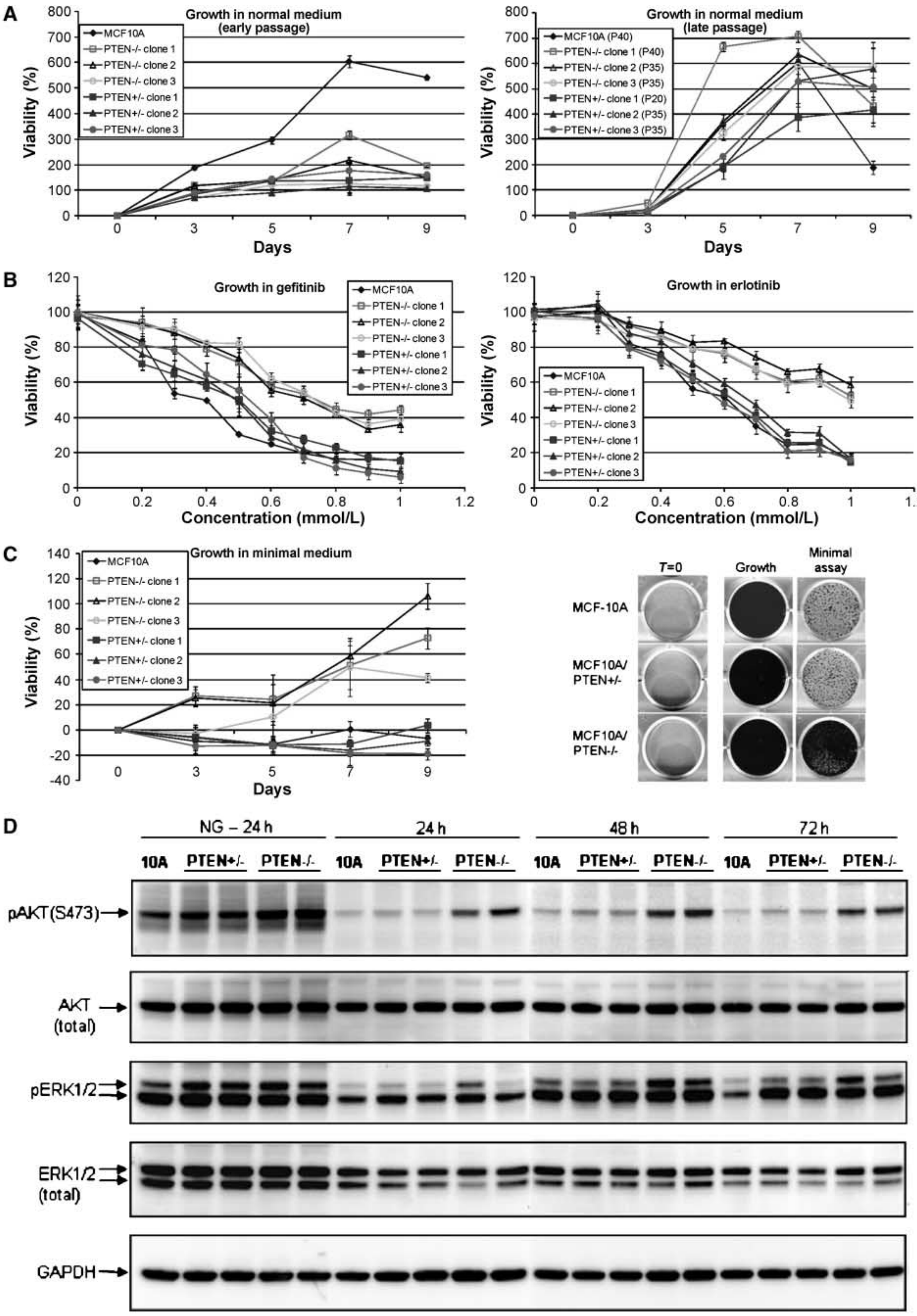
A
Growth in normal medium (early passage)
Viability (%)
Days
0
100
200
300
400
500
600
700
800
0
3
5
7
9
MCF10A
PTEN-/- clone 1
PTEN-/- clone 2
PTEN-/- clone 3
PTEN+/- clone 1
PTEN+/- clone 2
PTEN+/- clone 3
Growth in normal medium (late passage)
MCF10A (P40)
PTEN-/- clone 1 (P40)
PTEN-/- clone 2 (P35)
PTEN-/- clone 3 (P35)
PTEN+/- clone 1 (P20)
PTEN+/- clone 2 (P35)
PTEN+/- clone 3 (P35)
B
Growth in gefitinib
Growth in erlotinib
Viability (%)
Concentration (mmol/L)
0
20
40
60
80
100
120
0.2
0.4
0.6
0.8
1
1.2
C
Growth in minimal medium
Viability (%)
Days
-40
-20
0
20
40
60
80
100
120
140
T=0
Growth
Minimal assay
MCF-10A
MCF10A/ PTEN+/-
MCF10A/ PTEN-/-
D
NG – 24 h
24 h
48 h
72 h
10A
PTEN+/-
PTEN-/-
pAKT(S473)
AKT (total)
pERK1/2
ERK1/2 (total)
GAPDH

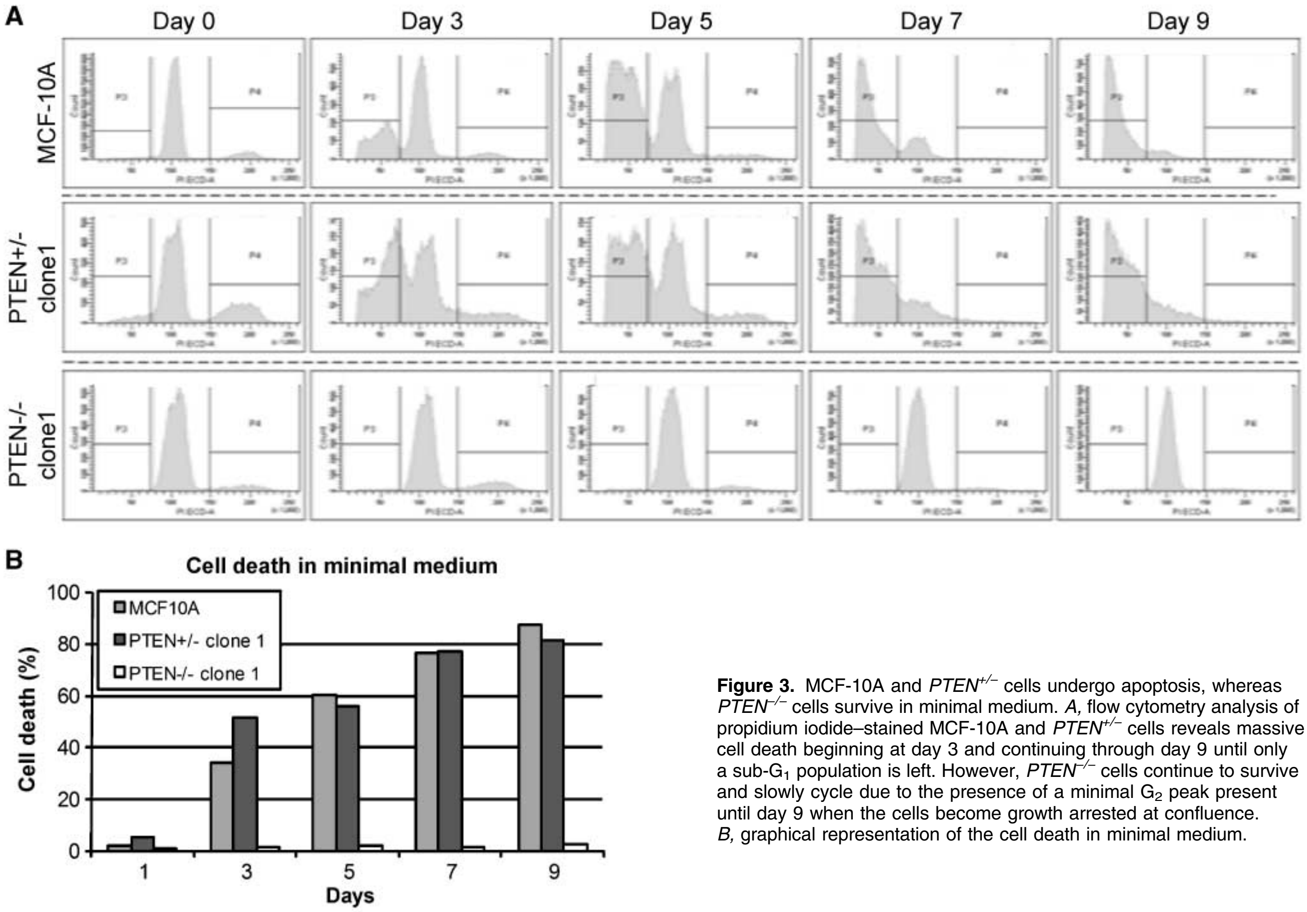

**Figure 3.** MCF-10A and *PTEN*$^{+/-}$ cells undergo apoptosis, whereas *PTEN*$^{-/-}$ cells survive in minimal medium. *A,* flow cytometry analysis of propidium iodide–stained MCF-10A and *PTEN*$^{+/-}$ cells reveals massive cell death beginning at day 3 and continuing through day 9 until only a sub-$G_1$ population is left. However, *PTEN*$^{-/-}$ cells continue to survive and slowly cycle due to the presence of a minimal $G_2$ peak present until day 9 when the cells become growth arrested at confluence. *B,* graphical representation of the cell death in minimal medium.

studies, as a control for resistance to cell rounding and anoikis, were MCF-10A cells overexpressing the antiapoptotic gene Bcl2 (8). PARP cleavage, an indicator of apoptosis, was examined after the cells were treated with latrunculin-A to induce cell rounding (Fig. 5*A*). Latrunculin-A is a specific inhibitor of actin polymerization that has been used to induce rapid rounding of MCF-10A cells while allowing the cells to maintain attachment to the tissue culture dishes (8). MCF-10A, *PTEN*$^{+/-}$, and *PTEN*$^{-/-}$ cells treated with vehicle control in minimal assay medium showed similar, low levels of PARP cleavage. MCF-10A.Bcl2 cells, with verified resistance to apoptosis, had undetectable PARP cleavage. On addition of latrunculin-A, the MCF-10A parent line and *PTEN*$^{+/-}$ clones undergo significant PARP cleavage, whereas *PTEN*$^{-/-}$ cells maintain high levels of full-length PARP, similar to that of MCF-10A.Bcl2 cells. To examine whether *PTEN*$^{-/-}$ cells exhibited a general resistance to apoptosis, all cells were treated with the death receptor ligand, tumor necrosis factor–related apoptosis-inducing ligand (TRAIL). Binding of TRAIL to transmembrane death receptors stimulates apoptosis via the extrinsic pathway, which is independent of AKT and the mitochondria. Within 2 h of TRAIL-related apoptosis inducing ligand treatment, all MCF-10A cells and variants began to undergo apoptosis confirmed by the increase of cleaved PARP levels. The apoptotic resistance of *PTEN*$^{-/-}$ cells therefore seems restricted to the intrinsic apoptosis pathway, because it cannot prevent apoptosis that occurs downstream of mitochondrial apoptosis signaling. Additionally, to determine anoikis resistance, the cells were plated over low-attachment plates. Without tissue culture–treated plastic, the cells remained in suspension. After detachment for 24 h, MCF-10A parental cells and *PTEN*$^{+/-}$ clones undergo massive cell death as shown by high levels of cleaved PARP and the presence of a sub-$G_1$ peak (Fig. 5*B* and *C*). *PTEN*$^{-/-}$ cells maintained high levels of full-length PARP and a lower percentage of cells in sub-$G_1$, indicating their resistance to anoikis. pERK levels are only very slightly elevated in *PTEN*$^{+/-}$ clones; these cells maintained similar levels of PARP cleavage to the parental cells. Although the first *PTEN*$^{-/-}$ clone revealed an increase in pERK levels compared with the other *PTEN*$^{-/-}$ clone, no differences in the levels

**Figure 2.** PTEN loss confers growth in minimal medium. *A,* early- and late-passage growth of MCF-10A cells and *PTEN*$^{+/-}$ and *PTEN*$^{-/-}$ clones in normal MCF-10A growth medium. *Points,* mean of two independent experiments done in quadruplicate; *bars,* SD. *B,* cell growth of MCF-10A cells and *PTEN*$^{+/-}$ and *PTEN*$^{-/-}$ clones after exposure to increasing doses of the EGF receptor antagonists gefitinib and erlotinib. *Points,* mean of three independent experiments done in quadruplicate; *bars,* SD. *C,* cell growth in minimal medium. *Points,* mean of two independent experiments done in quadruplicate; *bars,* SD. On day 6, MCF-10A, *PTEN*$^{+/-}$, and *PTEN*$^{-/-}$ cells were fixed and stained with a solution of 10% PBS-buffered formalin and 0.25% crystal violet. Representative wells from MCF-10A, *PTEN*$^{+/-}$, and *PTEN*$^{-/-}$ cells are shown. *D,* MCF-10A, two *PTEN*$^{+/-}$, and two *PTEN*$^{-/-}$ clones were plated in either normal growth medium (*NG*) or minimal assay medium and harvested at the indicated times by direct addition of radioimmunoprecipitation assay lysis buffer.

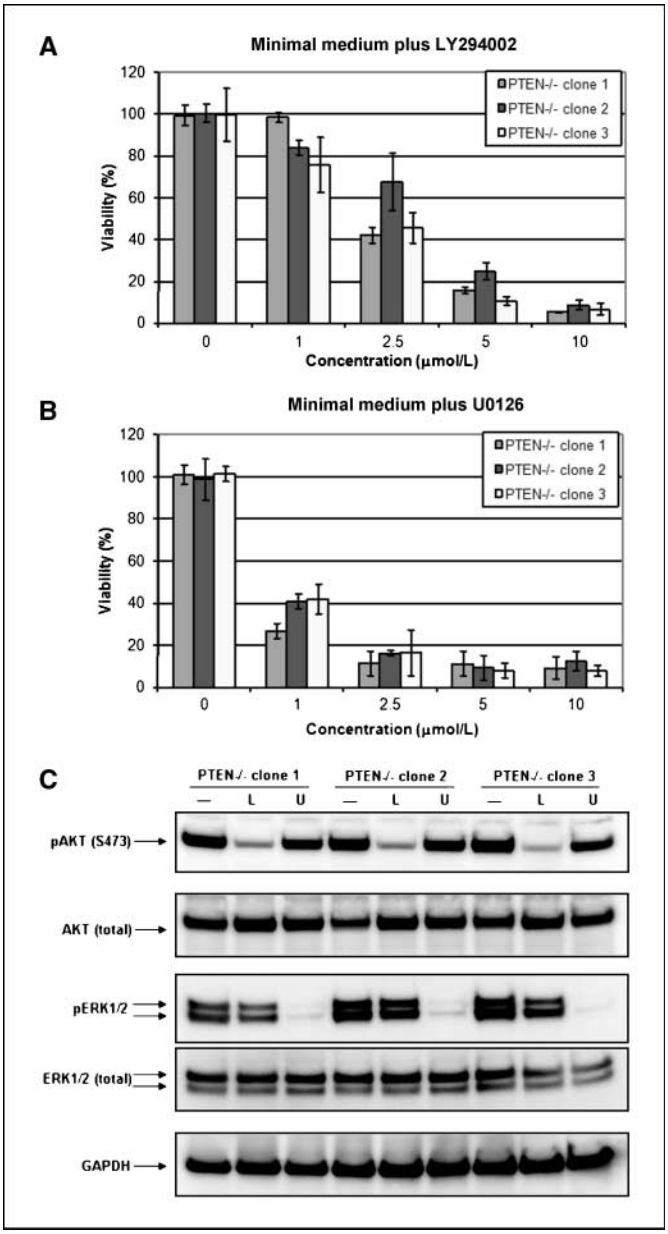

**Figure 4.** Inhibition of the PI3K and MAPK pathways suppresses proliferation in minimal medium of *PTEN*$^{-/-}$ MECs. *A,* percent growth of three *PTEN*$^{-/-}$ clones in minimal assay medium with increasing concentrations of LY294002. *B,* percent growth of three *PTEN*$^{-/-}$ clones in minimal assay medium with increasing concentrations of U0126. *C,* three *PTEN*$^{-/-}$ clones were plated in minimal assay medium and allowed to recover overnight. The next day, fresh minimal assay medium was added with or without 10 μmol/L LY294002 (*L*) or 10 μmol/L U0126 (*U*) for 1 h. Western blot analysis showing pAKT reduction in the cells treated with the PI3K inhibitor LY294002 and pERK reduction in the cells treated with the MEK inhibitor U0126.

of cleaved PARP were observed between clones. Therefore, whereas MEK activation was required for continued cell growth (Fig. 4), the levels of ERK activation were relatively independent from apoptosis during detachment. It is more likely that AKT activation was responsible for the resistance to anoikis, because high levels of pAKT were maintained in the suspended *PTEN*$^{-/-}$ cells.

**PTEN loss sensitizes cells to the chemotherapeutic drug doxorubicin but not paclitaxel.** Studies suggest that loss of PTEN expression correlate with poor prognosis as well as resistance to chemotherapies (21, 22). To determine whether PTEN loss mediates chemotherapeutic resistance and increases cell survival, the PTEN isogenic MCF-10A cells were exposed to increasing concentrations of doxorubicin and paclitaxel. Primary normal breast epithelial cells are alive and metabolizing but not actively proliferating. To mimic healthy, growth-arrested epithelial cells, MCF-10A cells were plated at high density ($1.5 \times 10^4$) per well in a 96-well plate in minimal assay medium. After 24 h, the cells attached as ~90% confluent monolayer. Although *PTEN*$^{-/-}$ cells have the ability to grow in minimal medium, they remain contact-inhibited and growth-arrested at confluence; therefore, the plating densities used matched those of the MCF-10A parental cells. Drugs were added after growth arrest to determine cell survival. Interestingly, *PTEN*$^{+/-}$ and *PTEN*$^{-/-}$ cells responded differently to the drugs. Doxorubicin similarly reduced the percentage of surviving cells in both *PTEN*$^{+/-}$ and *PTEN*$^{-/-}$ cells (Fig. 6*A*). Even at the low concentration of 5 nmol/L, doxorubicin reduced *PTEN*$^{+/-}$ and *PTEN*$^{-/-}$ clones by 10% and 24%, respectively. No difference in susceptibility was observed between the isogenic cells following exposure to paclitaxel (Fig. 6*B*).

## Discussion

The loss of PTEN expression or the acquisition of activating PI3K mutations (*PIK3CA*) occurs in ~50% to 75% of breast cancers, illustrating the importance of the PI3K pathway in breast cancer. Notably, loss of PTEN expression and *PIK3CA* mutation are mutually exclusive events (23) likely because PTEN and PI3K exist in a tight, regulatory loop, strictly controlling phosphatidylinositol levels. The loss of PTEN or the acquisition of an activating mutation in *PIK3CA* are reciprocal alterations, either of which would result in increased levels of phosphatidylinositol 3,4,5-trisphosphate and remove the selective pressure to convert phosphatidylinositol 3,4,5-trisphosphate to its phosphatidylinositol 4,5-bisphosphate counterpart. Our findings support the role of PTEN loss in breast cancer based on the ability of *PTEN*$^{-/-}$ cells to proliferate in the absence of growth factors and their resistance to anoikis. However, PTEN loss is insufficient to promote active tumorigenesis of the MCF-10A cells, suggesting a need for other oncogenic events (24). This result is contradictory to recent data in which the overexpression of two clinically relevant PI3K mutations (H1047R and E545K) conferred anchorage-independent growth of MCF-10A cells in soft agar (25). However, in these studies, the expression of the *PIK3CA* mutant cDNA is under control of a cytomegalovirus promoter that may increase *PIK3CA* expression to levels not observed in primary tumors or derived cell lines. In support of this hypothesis, knockin of the same *PIK3CA* activating mutations, H1074R and E545K, did not cause anchorage-independent growth of MCF-10A cells (26). Similar to MCF-10A *PTEN*$^{-/-}$ cells, knockin mutant *PIK3CA* cells were not tumorigenic, did not form colonies in soft agar, and did not alter acinar growth in three-dimensional Matrigel culture.

Although metastasis is the cause of 90% of human cancer deaths (27), the metastatic process presents numerous challenges to tumor cells, including apoptosis that results from detachment (anoikis) or cell shape change (amorphosis; ref. 28). Resistance to apoptosis allows tumor cells to survive these challenges (29) but does not promote immediate tumor outgrowth at the secondary site, yielding a period of tumor dormancy (30). There is currently tremendous clinical interest in such dormant tumor cells, because their presence in the bloodstream strongly predicts poor patient outcome in breast cancer (31, 32). The importance of defining the mechanisms that promote tumor dormancy is also emphasized by the observation that breast tumor patients who are diagnosed early with no detectable regional metastases have >30% chance of recurrence when followed for 10 to 15 years (33, 34). Our results indicate that PTEN loss induces a dormant tumor cell phenotype by promoting resistance to apoptosis without inducing complete anchorage-independent growth. Recent evidence shows that MECs that have not fully transformed to anchorage-independent growth are still fully capable of metastasizing to the lung in a dormant state and then recurring once growth-initiating oncogenes are activated (35, 36). Systems based on fibroblasts or exogenous overexpression of *PI3KCA* display active tumor growth, whereas our system based on homologous knockout of *PTEN* in MCF-10A MECs more effectively models the dormant phenotype of carcinoma cells. However, such dormant tumor cells are typically difficult to treat with traditional chemotherapies, because they persist without active cell division. Defining which types of chemotherapy are able to effectively target tumor cells in such a dormant state will be critical to treating metastatic recurrence.

A variety of chemotherapeutic agents converge on a common final pathway leading to apoptotic cell death. Certain studies have shown that activation of the PI3K pathway enhances the survival of cancer cells in response to such agents and contribute

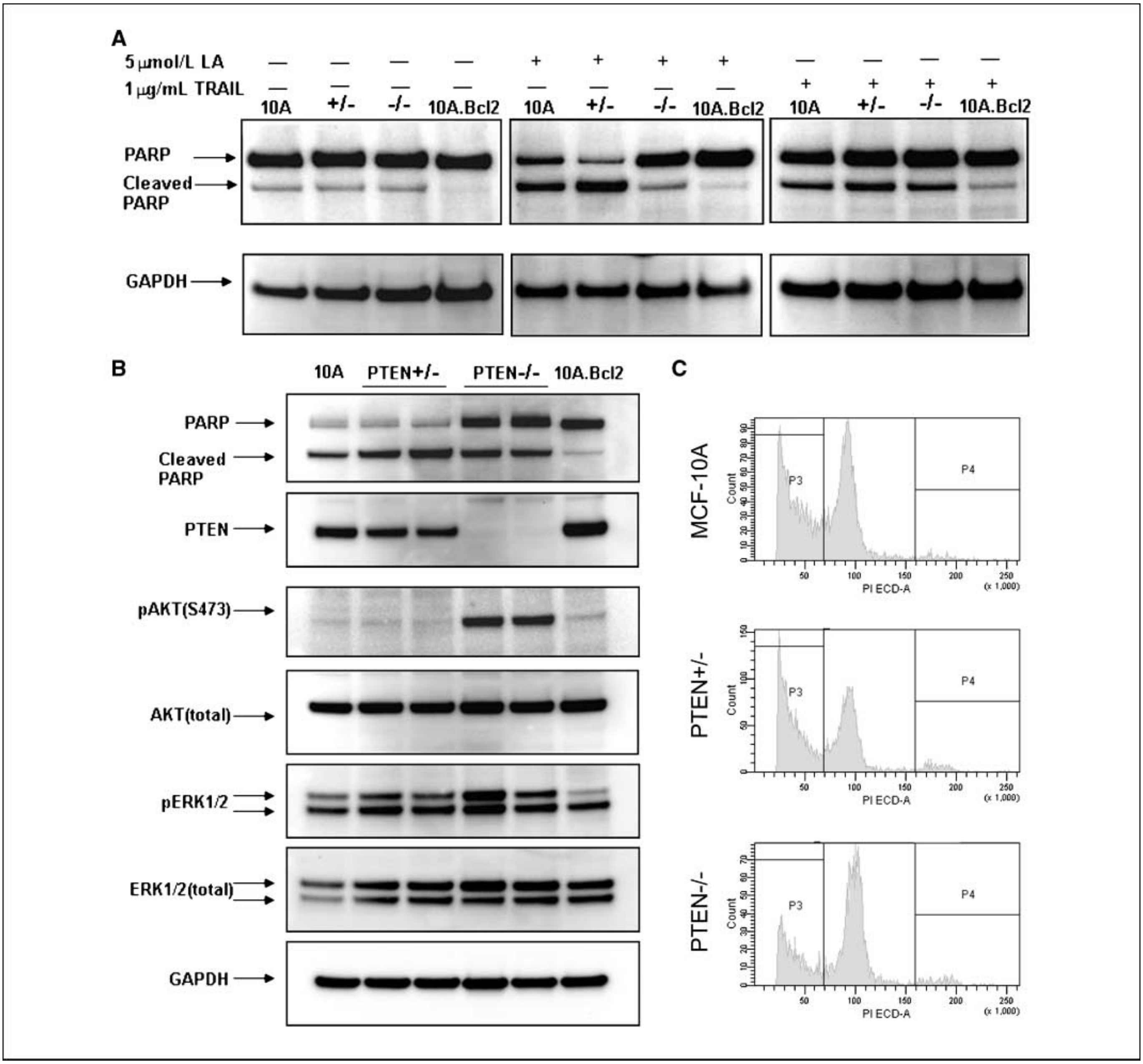

**Figure 5.** PTEN loss promotes resistance to apoptosis on cell rounding and anoikis. *A,* MCF-10A, a *PTEN*$^{+/-}$ clone, a *PTEN*$^{-/-}$ clone, and MCF-10A.Bcl2 cells were plated in minimal assay medium. The next day, the medium was changed to fresh minimal medium with or without 5 µmol/L latrunculin-A (*LA*) to induce cell rounding for 24 h or 1 µg/mL TRAIL for 2 h and harvested at the indicated times by direct addition of radioimmunoprecipitation assay lysis buffer. *B,* MCF-10A, two representative *PTEN*$^{+/-}$ clones, two representative *PTEN*$^{-/-}$ clones, and MCF-10A.Bcl2 cells were incubated in suspension in normal growth medium for 24 h. *C,* flow cytometry analysis of MCF-10A, *PTEN*$^{+/-}$ clone 1, and *PTEN*$^{-/-}$ clone 1 incubated in suspension in DMEM/F-12 for 24 h. A larger percentage of MCF-10A (42.8%) and *PTEN*$^{+/-}$ cells (49.4%) undergo apoptosis than *PTEN*$^{-/-}$ cells (29.6%).

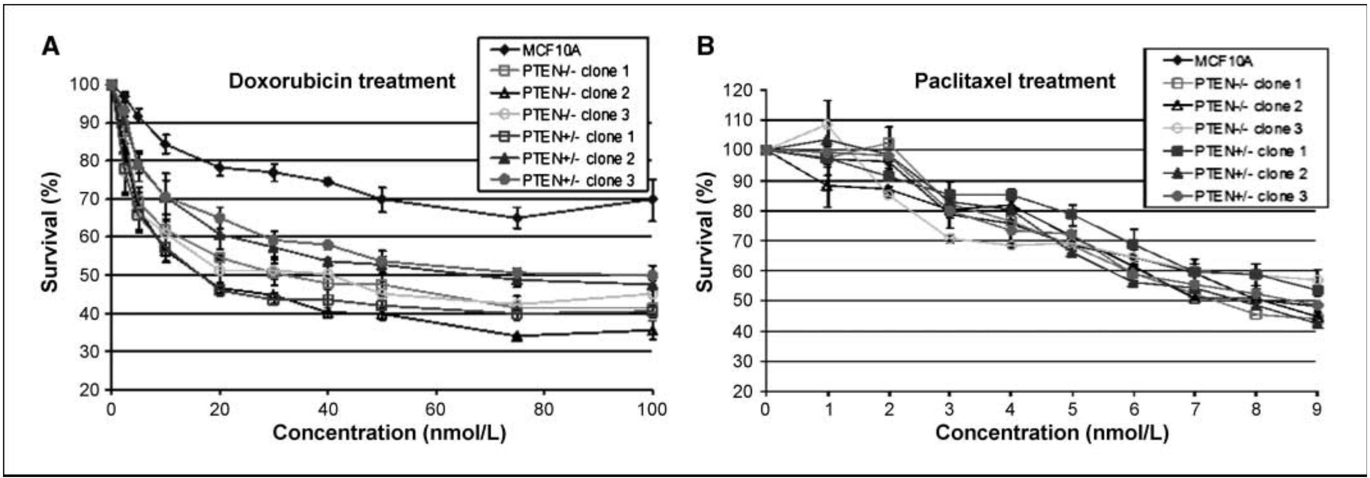

**Figure 6.** PTEN loss sensitizes MECs to the commonly used breast cancer chemotherapeutic doxorubicin but not to paclitaxel. Cell growth of MCF-10A cells and *PTEN*$^{+/-}$ and *PTEN*$^{-/-}$ clones after exposure to increasing doses of doxorubicin (*A*) and paclitaxel (*B*). *Points,* mean of three independent experiments done in quadruplicate; *bars,* SD.

to chemotherapy resistance. However, these previous studies employed an overexpressed, constituently active AKT1 (37, 38), which may not recapitulate the physiologically active AKT levels due to PTEN loss or *PIK3CA* mutations, whereas other studies overexpressed an oncogene such as constitutively active Ras (39) or HER-2 (40) in the MCF-7 breast adenocarcinoma line, which already contains a PIK3CA mutation (E545K; ref. 41). Here, to more closely recapitulate physiologic levels of active AKT, we used the MCF-10A isogenic PTEN knockout clones to determine chemotherapeutic response to doxorubicin and paclitaxel. Surprisingly, *PTEN*$^{-/-}$ clones were more susceptible to doxorubicin than their parental PTEN-expressing counterparts. However, no difference in survival was observed between the isogenic clones when treated with paclitaxel. The susceptibility of *PTEN*$^{+/-}$ and *PTEN*$^{-/-}$ cells to doxorubicin and not paclitaxel may be explained by the different mechanisms of action of each drug. Paclitaxel is a microtubule-stabilizing compound that interferes with the normal breakdown of this cytoskeletal component. This drug immediately and adversely affects cell function as microtubule-inherent dynamic instability is necessary for their function to transport other cellular components. Doxorubicin is known to intercalate within the DNA and inhibition of topoisomerase II progression, eliciting DNA damage. On DNA damage, normal cells undergo growth arrest to either repair the damage or undergo apoptosis if the damage is substantial. However, constitutively active PI3K and pathway components have been shown to override DNA damage–induced cell arrest (42–44). Haploinsufficiency and deletion of PTEN may allow for cell cycle progression and death due to massive DNA damage. Further work to elucidate the mechanisms by which PTEN expression loss may contribute to chemotherapy susceptibility is warranted.

There is a significant clinical relevance for the creation and characterization of this PTEN isogenic model system. Using this model, we have shown that PTEN expression loss in MECs results in constitutive AKT activation and induces multiple phenotypic alterations characteristic of breast tumor cells, including growth factor–independent proliferation and protection from anoikis. PTEN expression loss also confers increased susceptibility to doxorubicin but not paclitaxel. Together, these data support the notion that the cancer-associated PTEN expression loss may significantly contribute to breast cancer cell survival and tumor dormancy.

## Disclosure of Potential Conflicts of Interest

No potential conflicts of interest were disclosed.

## Acknowledgments

Received 3/23/09; revised 8/4/09; accepted 9/2/09; published OnlineFirst 10/20/09.

**Grant support:** Maryland Cigarette Restitution Fund (K.E. Bachman), Susan G. Komen Breast Cancer Foundation grant PDF104506 (M.I. Vitolo), National Cancer Institute grants T32-DK067872 (M.B. Weiss), R01-CA115699 (T. Waldman), and R01-CA124704 (S.S. Martin), Breast Cancer Research Foundation (B.H. Park), and National Cancer Institute and General Medicine/NIH grants R01-CA107331 and R01 GM58888 (D.J. Weber).

The costs of publication of this article were defrayed in part by the payment of page charges. This article must therefore be hereby marked *advertisement* in accordance with 18 U.S.C. Section 1734 solely to indicate this fact.

We thank Agnes Cheung for developing the MCF-10A.Bcl2 cell line and Regina Harley for flow cytometry experiments.

## References

1. Bruni P, Boccia A, Baldassarre G, et al. PTEN expression is reduced in a subset of sporadic thyroid carcinomas: evidence that PTEN-growth suppressing activity in thyroid cancer cells mediated by p27$^{kip1}$. Oncogene 2000;19:3146–55.
2. Depowski PL, Rosenthal SI, Ross JS. Loss of expression of the PTEN gene protein product is associated with poor outcome in breast cancer. Mod Pathol 2001;14:672–6.
3. Ebert MP, Fei G, Schandl L, et al. Reduced PTEN expression in the pancreas overexpressing transforming growth factor-β1. Br J Cancer 2002;86:257–62.
4. Kurose K, Zhou XP, Araki T, Cannistra SA, Maher ER, Eng C. Frequent loss of PTEN expression is linked to elevated phosphorylated Akt levels, but not associated with p27 and cyclin D1 expression, in primary epithelial ovarian carcinomas. Am J Pathol 2001;158:2097–106.
5. Perren A, Weng LP, Boag AH, et al. Immunohistochemical evidence of loss of PTEN expression in primary ductal adenocarcinomas of the breast. Am J Pathol 1999;155:1253–60.
6. Liaw D, Marsh DJ, Li J, et al. Germline mutations of the PTEN gene in Cowden disease, an inherited breast and thyroid cancer syndrome. Nat Genet 1997;16:64–7.
7. Marsh DJ, Zheng Z, Zedenius J, et al. Differential loss of heterozygosity in the region of the Cowden locus within 10q22-23 in follicular thyroid adenomas and carcinomas. Cancer Res 1997;57:500–3.

**8.** Martin SS, Leder P. Human MCF10A mammary epithelial cells undergo apoptosis following actin depolymerization that is independent of attachment and rescued by Bcl-2. Mol Cell Biol 2001;21:6529–36.

**9.** Pinkas J, Martin SS, Leder P. Bcl-2-mediated cell survival promotes metastasis of EpH4 βMEKDD mammary epithelial cells. Mol Cancer Res 2004;2:551–6.

**10.** Lee C, Kim JS, Waldman T. PTEN gene targeting reveals a radiation-induced size checkpoint in human cancer cells. Cancer Res 2004;64:6906–14.

**11.** Topaloglu O, Hurley PJ, Yildirim O, Civin CI, Bunz F. Improved methods for the generation of human gene knockout and knockin cell lines. Nucleic Acids Res 2005;33:e158.

**12.** Rago C, Vogelstein B, Bunz F. Genetic knockouts and knockins in human somatic cells. Nat Protoc 2007;2:2734–46.

**13.** Garcia JM, Silva J, Pena C, et al. Promoter methylation of the PTEN gene is a common molecular change in breast cancer. Genes Chromosomes Cancer 2004;41:117–24.

**14.** Liang J, Slingerland JM. Multiple roles of the PI3K/PKB (Akt) pathway in cell cycle progression. Cell Cycle 2003;2:339–45.

**15.** Hanahan D, Weinberg RA. The hallmarks of cancer. Cell 2000;100:57–70.

**16.** Vranic S, Bilalovic N, Lee LM, Kruslin B, Lilleberg SL, Gatalica Z. PIK3CA and PTEN mutations in adenoid cystic carcinoma of the breast metastatic to kidney. Hum Pathol 2007;38:1425–31.

**17.** Janssen EA, Soiland H, Skaland I, et al. Comparing the prognostic value of PTEN and Akt expression with the mitotic activity index in adjuvant chemotherapy-treated node-negative breast cancer patients aged <55 years. Cell Oncol 2007;29:25–35.

**18.** Schmitz M, Grignard G, Margue C, et al. Complete loss of PTEN expression as a possible early prognostic marker for prostate cancer metastasis. Int J Cancer 2007;120:1284–92.

**19.** Shin SI, Freedman VH, Risser R, Pollack R. Tumorigenicity of virus-transformed cells in nude mice is correlated specifically with anchorage independent growth *in vitro*. Proc Natl Acad Sci U S A 1975;72:4435–9.

**20.** Khwaja A, Rodriguez-Viciana P, Wennstrom S, Warne PH, Downward J. Matrix adhesion and Ras transformation both activate a phosphoinositide 3-OH kinase and protein kinase B/Akt cellular survival pathway. EMBO J 1997;16:2783–93.

**21.** Campbell RA, Bhat-Nakshatri P, Patel NM, Constantinidou D, Ali S, Nakshatri H. Phosphatidylinositol 3-kinase/AKT-mediated activation of estrogen receptor α: a new model for anti-estrogen resistance. J Biol Chem 2001;276:9817–24.

**22.** Garcia JM, Silva JM, Dominguez G, et al. Allelic loss of the PTEN region (10q23) in breast carcinomas of poor pathophenotype. Breast Cancer Res Treat 1999;57:237–43.

**23.** Saal LH, Holm K, Maurer M, et al. PIK3CA mutations correlate with hormone receptors, node metastasis, and ERBB2, and are mutually exclusive with PTEN loss in human breast carcinoma. Cancer Res 2005;65:2554–9.

**24.** Ciardiello F, Gottardis M, Basolo F, et al. Additive effects of c-erbB-2, c-Ha-ras, and transforming growth factor-α genes on *in vitro* transformation of human mammary epithelial cells. Mol Carcinog 1992;6:43–52.

**25.** Isakoff SJ, Engelman JA, Irie HY, et al. Breast cancer-associated PIK3CA mutations are oncogenic in mammary epithelial cells. Cancer Res 2005;65:10992–1000.

**26.** Gustin JP, Karakas B, Weiss MB, et al. Knockin of mutant PIK3CA activates multiple oncogenic pathways. Proc Natl Acad Sci U S A 2009;106:2835–40.

**27.** Weigelt B, Peterse JL, van't Veer LJ. Breast cancer metastasis: markers and models. Nat Rev Cancer 2005;5:591–602.

**28.** Martin SS, Vuori K. Regulation of Bcl-2 proteins during anoikis and amorphosis. Biochim Biophys Acta 2004;1692:145–57.

**29.** Mehlen P, Puisieux A. Metastasis: a question of life or death. Nat Rev Cancer 2006;6:449–58.

**30.** Martin SS, Ridgeway AG, Pinkas J, et al. A cytoskeleton-based functional genetic screen identifies Bcl-xL as an enhancer of metastasis, but not primary tumor growth. Oncogene 2004;23:4641–5.

**31.** Riethdorf S, Wikman H, Pantel K. Review: biological relevance of disseminated tumor cells in cancer patients. Int J Cancer 2008;123:1991–2006.

**32.** Riethmuller G, Klein CA. Early cancer cell dissemination and late metastatic relapse: clinical reflections and biological approaches to the dormancy problem in patients. Semin Cancer Biol 2001;11:307–11.

**33.** Fisher B, Jeong JH, Dignam J, et al. Findings from recent National Surgical Adjuvant Breast and Bowel Project adjuvant studies in stage I breast cancer. J Natl Cancer Inst Monogr 2001;:62–6.

**34.** Wallgren A, Bonetti M, Gelber RD, et al. Risk factors for locoregional recurrence among breast cancer patients: results from International Breast Cancer Study Group Trials I through VII. J Clin Oncol 2003;21:1205–13.

**35.** Podsypanina K, Du YC, Jechlinger M, Beverly LJ, Hambardzumyan D, Varmus H. Seeding and propagation of untransformed mouse mammary cells in the lung. Science 2008;321:1841–4.

**36.** Weinberg RA. Leaving home early: reexamination of the canonical models of tumor progression. Cancer Cell 2008;14:283–4.

**37.** Schmidt M, Hovelmann S, Beckers TL. A novel form of constitutively active farnesylated Akt1 prevents mammary epithelial cells from anoikis and suppresses chemotherapy-induced apoptosis. Br J Cancer 2002;87:924–32.

**38.** VanderWeele DJ, Zhou R, Rudin CM. Akt up-regulation increases resistance to microtubule-directed chemotherapeutic agents through mammalian target of rapamycin. Mol Cancer Ther 2004;3:1605–13.

**39.** Jin W, Wu L, Liang K, Liu B, Lu Y, Fan Z. Roles of the PI-3K and MEK pathways in Ras-mediated chemoresistance in breast cancer cells. Br J Cancer 2003;89:185–91.

**40.** Knuefermann C, Lu Y, Liu B, et al. HER2/PI-3K/Akt activation leads to a multidrug resistance in human breast adenocarcinoma cells. Oncogene 2003;22:3205–12.

**41.** Bachman KE, Argani P, Samuels Y, et al. The PIK3CA gene is mutated with high frequency in human breast cancers. Cancer Biol Ther 2004;3:772–5.

**42.** Kandel ES, Skeen J, Majewski N, et al. Activation of Akt/protein kinase B overcomes a G(2)/m cell cycle checkpoint induced by DNA damage. Mol Cell Biol 2002;22:7831–41.

**43.** Zhan Q, Antinore MJ, Wang XW, et al. Association with Cdc2 and inhibition of Cdc2/Cyclin B1 kinase activity by the p53-regulated protein Gadd45. Oncogene 1999;18:2892–900.

**44.** Shtivelman E, Sussman J, Stokoe D. A role for PI 3-kinase and PKB activity in the $G_2$/M phase of the cell cycle. Curr Biol 2002;12:919–24.